

Technical Note

Presence of Solid $\text{Fe}(\text{OH})_2$ in EMF-pH Diagram for Iron*

DAVID C. SILVERMAN*

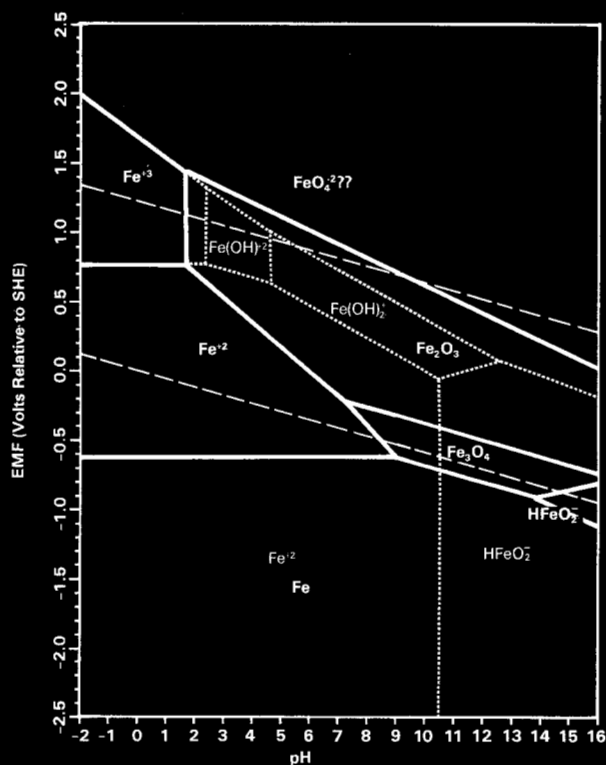


FIGURE 1 — EMF-pH diagram for iron as calculated by Pourbaix.¹ Temperature is 298 K. All ions are at an activity of 10^{-6} .

Much of the calculated EMF-pH (Pourbaix) diagram for iron originally derived by Pourbaix is consistent with actual experimental observations of immunity, passivity, and corrosion versus potential and pH.¹ An example of this original diagram at 298 K, 10^{-6} ionic activity is shown in Figure 1. The compounds originally considered by Pourbaix are shown in Table 1.

However, one portion of the diagram that disagrees with experimental observation is the prediction that the area of stability of metallic iron lies adjacent to the area of stability of Fe_3O_4 under mildly alkaline conditions. This discrepancy was pointed out by Pourbaix in his discussion of the diagram.¹ He noted that, whereas Figure 1 predicts that in the absence of oxygen iron may be taken directly from immunity to passivity (Fe to Fe_3O_4) by increasing potential, experimental results have indicated that an area of "weak" corrosion actually lies

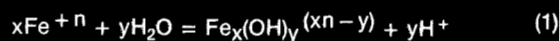
TABLE 1 — Compounds Considered by Pourbaix for Iron¹

Compound	Free Energy of Formation (joule/mole)
Fe	0.0
Fe_3O_4 (anhydrous)	-1.01×10^6
Fe_2O_3 (anhydrous)	-7.40×10^5
Fe_2O_3 (hydrrous - $\text{Fe}(\text{OH})_3$)	-6.89×10^5
FeO (hydrrous - $\text{Fe}(\text{OH})_2$)	-2.46×10^5
Fe^{+2}	-8.49×10^4
HFeO_2^-	-3.79×10^5
Fe^{+3}	-1.05×10^4
FeOH^{+2}	-2.34×10^5
$\text{Fe}(\text{OH})_2^+$	-4.44×10^5
FeO_4^{-2} (?)	-4.67×10^5

between these two regions. The compound Fe_3O_4 is not expected to exhibit such corrosion. In addition, this prediction would mean that iron in a +3 state could be in direct equilibrium with iron with no charge at relatively cathodic potentials. No iron corrosion mechanism in aqueous environments suggests this possibility.²

The original thermodynamic diagram as calculated by Pourbaix contains a large number of approximations in the predicted free energies of formation, especially for the ions. A number of presently accepted aqueous iron compounds and ions were omitted from the original consideration. To correct this deficiency, the EMF-pH (Pourbaix) diagram for iron has been rederived using newer, more reliable thermodynamic values based on data presented by Baes and Mesmer.³ The purpose of this rederivation is to show that by using this data, the iron diagram is modified to contain a new region of solid $\text{Fe}(\text{OH})_2$ lying between Fe and Fe_3O_4 . This region could correspond to the region of weak corrosion originally discussed by Pourbaix.

The compounds considered in the derivation of the diagram are shown in Table 2. The free energies of formation of all of the solid species and of the ions Fe^{+2} and Fe^{+3} are from Naumov, *et al.*⁴ The free energies of formation of the other dissolved species have been calculated by combining the above values for Fe^{+2} and Fe^{+3} , the free energy of formation of water (-2.37×10^5 joule/mole) and the hydrolysis constants as estimated by Baes and Mesmer for the reaction



where $n = 2$ or 3 .

Baes and Mesmer correct the hydrolysis constants to zero ionic strength. In addition, these authors estimate the standard state entropy changes for these hydrolysis reac-

*Submitted for publication January, 1982; revised February, 1982.

*Monsanto Company, St. Louis, Missouri.

TABLE 2 — Compounds Considered in New Diagram for Iron

Compound	Free Energy of Formation (298K) (joule/mole)	Standard Entropy (298K) (joule/mole-K)	Ref.
Fe	0.0	2.71×10	4
Fe ₃ O ₄	-1.02×10^6	1.46×10^2	4
Fe ₂ O ₃	-7.42×10^5	8.73×10	4
FeOOH	-4.90×10^5	6.73×10	4
Fe(OH) ₂ Solid	-4.93×10^5	9.24×10	4
Fe(OH) ₃ Solid	-7.14×10^5	9.61×10	4
Fe ⁺²	-9.22×10^4	-1.07×10^2	4
FeOH ⁺	-2.74×10^5	-2.93×10	3
Fe(OH) ₂ Dissolved	-4.49×10^5	3.80×10	3
Fe(OH) ₃ ⁻	-6.21×10^5	4.18×10	3
Fe ⁺³	-1.78×10^4	-2.79×10^2	4
FeOH ⁺²	-2.42×10^5	-1.05×10^2	3
Fe(OH) ₂ ⁺	-4.59×10^5	-2.93×10	3
Fe(OH) ₃ Dissolved	-6.61×10^5	7.52×10	3
Fe(OH) ₄ ⁻	-8.43×10^5	2.51×10	3
Fe ₂ (OH) ₂ ⁺⁴	-4.94×10^5	-2.93×10^2	3
Fe ₃ (OH) ₄ ⁺⁵	-9.69×10^5	-4.64×10^2	3
FeO ₄ ⁻² (?)	-4.67×10^5	3.76×10	1,13

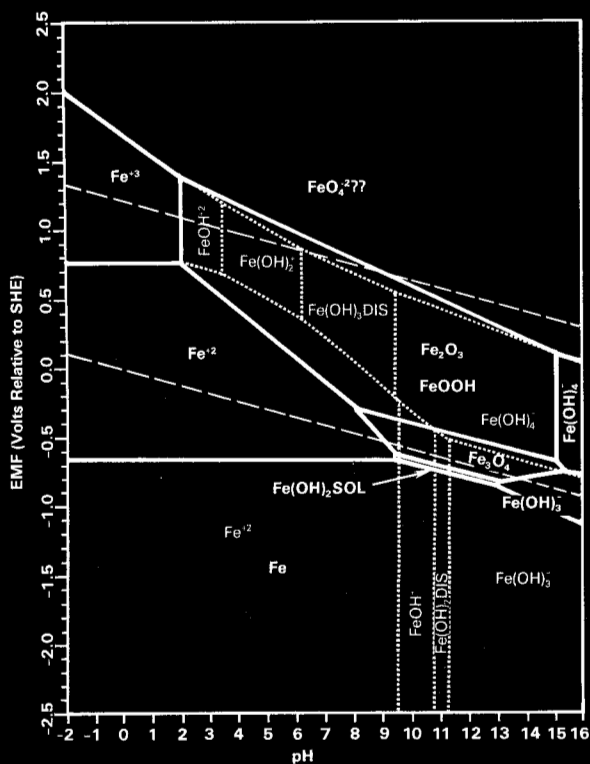


FIGURE 2 — EMF-pH diagram for iron as calculated from the data in Table 2. Temperature is 298 K. All ions are at an activity of 10^{-6} . Note that Fe₂O₃ and FeOOH have similar stabilities.

using the algorithm of Fronig, Shanley, and Verink.⁵ The temperature is 298 K. For simplicity, all ionic species have been assumed to be at 10^{-6} activity. Following Pourbaix, the ion FeO₄⁻² has been included with a question mark. There is evidence for the existence of FeO₄⁻² in aqueous basic solution, but it seems to be unstable in neutral or acid solutions.⁶

The important difference between Figures 1 and 2 is that a region of stability for solid Fe(OH)₂ now appears between the regions of stability for Fe and Fe₃O₄. At the assumed activities of 10^{-6} for the ions, a dissolved Fe(OH)₂ compound is also predicted to be the most stable state in the liquid phase in the lower potential region of the diagram centered around a pH of 11. The presence of this compound suggests that if formation of solid Fe(OH)₂ is kinetically favorable, a pathway of direct dissolution of solid Fe(OH)₂ to dissolved Fe(OH)₂ may be possible around a pH of 11. Solid Fe(OH)₂ has been described to be more soluble than the oxides Fe₂O₃, Fe₃O₄, and FeOOH.²

The formation of an uncharged dissolved Fe(OH)₂ species has been suggested by the data of both Sweeton and Baes⁷ and Tremaine and LeBlanc.⁸ In their experiments, the dependence of the measured equilibrium solubility of Fe₃O₄ was found to fit the scheme of soluble ferrous species Fe⁺², FeOH⁺, dissolved Fe(OH)₂, Fe(OH)₃⁻, and soluble ferric species dissolved Fe(OH)₃ and Fe(OH)₄⁻. Equilibrium constants were calculated for the formation of each species from Fe₃O₄. Tremaine and LeBlanc showed that the values of the free energies of formation of Fe⁺² and FeOH⁺ extrapolated from these results show substantial agreement with those values derived by other workers. These findings suggest that not only could uncharged, dissolved forms of hydrolyzed ferrous and ferric species exist but that, at least in dilute solution, they should be monomolecular as written.

In addition, both groups of workers include Fe(OH)₃⁻ and not HFeO₂⁻ as the dissolved ferrous ion species in strongly basic solution. The species Fe(OH)₃⁻ differs from HFeO₂⁻ by one water molecule. The ion Fe(OH)₃⁻ has been included in Figure 2 because Fe(OH)₃⁻ is consistent with the thermodynamic results and it does not break the sequence of each ferrous ion species being related to the one at higher pH by addition of one hydroxide ion.

Before one can conclude that solid Fe(OH)₂ is a stable species in the region predicted in Figure 2, surface characterization data is required at the potentials and pH cor-

tions. Thus, the standard state entropies of each of the ions can be calculated directly from the results of experimental measurements. The entropy data is included in Table 2.

The thermodynamic diagram based on the data in Table 2 is shown in Figure 2. The diagram was computer generated by

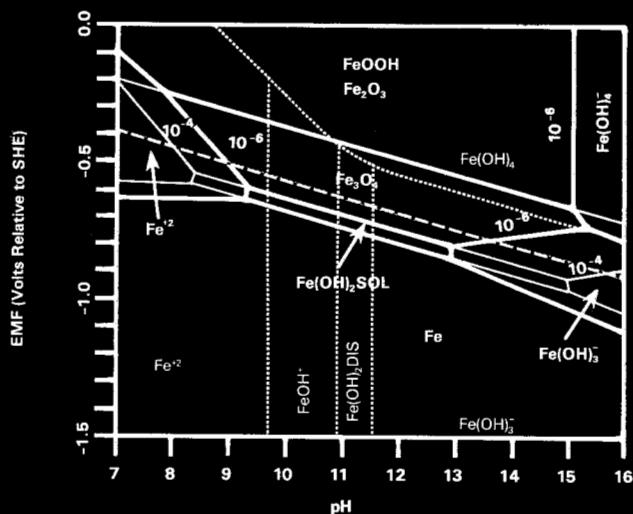


FIGURE 3 — Expanded view of EMF-pH diagram of iron at 298 K showing the effect of dissolved species activity (10^{-6} and 10^{-4}) in the vicinity of the $\text{Fe}(\text{OH})_2$ region of stability.

responding to the region. This data should at least be obtained under steady state conditions such that potential and pH are controlled within the proposed region of stability of $\text{Fe}(\text{OH})_2$. There is a paucity of such data especially between pH values of 9 and 13. However, some characterization data is available at pH greater than 14 though not necessarily obtained under steady state conditions.

To utilize this data, the diagram in Figure 2 was rederived at 10^{-4} activity for all ionic species. The portion of this diagram in the vicinity of the region of stability of $\text{Fe}(\text{OH})_2$ is shown in Figure 3. Included is the case of 10^{-6} activity for the ionic species. As shown, increasing the activity of the dissolved species expands the region of stability of $\text{Fe}(\text{OH})_2$ to higher and lower pH. Thus, the revised diagram predicts that solid $\text{Fe}(\text{OH})_2$ could be detectable above a pH of 14.

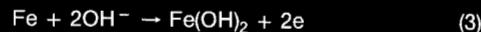
Mössbauer spectroscopy has been used to study the iron electrode during potential cycling in highly alkaline solutions of 5N KOH (pH > 14).⁹ From the results, phases of Fe, $\text{Fe}(\text{OH})_2$, and FeOOH were identified to be present during various stages of the charging process. The important point is that as cathodic charging occurs, FeOOH is converted to $\text{Fe}(\text{OH})_2$, some of which can then be converted to Fe. As shown in Figure 3, the thermodynamic diagram would suggest that as potential is changed in alkaline solutions, formation of an intermediate stable $\text{Fe}(\text{OH})_2$ phase between uncharged Fe and ionized Fe in the +3 state would be thermodynamically favorable. All that would be needed is a kinetic pathway to form the compound.

A number of workers have used cyclic voltammetry to study the charging process in alkaline solutions. At a pH of 14 or higher, a series of charge transfer peaks are observed as potential is scanned. Though there is disagreement as to the possible formation of Fe_3O_4 ,¹⁰⁻¹² most of these workers attribute one of the intermediate charge transfer processes to formation of $\text{Fe}(\text{OH})_2$ on the surface. In fact, Macdonald and Owen¹⁰ have shown that the measured second potential ar-

rests of the current peak attributed to $\text{Fe}(\text{OH})_2$ that appear in both the anodic and cathodic directions in 1 molar LiOH fulfill the inequality

$$E_c \leq E_{eq} \leq E_a \quad (2)$$

E_c and E_a are the second potential arrests measured during the reduction and oxidation of the surface respectively and E_{eq} is the equilibrium potential of the reaction



Fulfilling inequality (2) is a necessary condition if Equation (3) is to correspond to the potential of the peak to which it is attributed. Since the charge transfer processes involved in oxidizing and reducing surface iron species may be irreversible, the potential arrests may differ from the calculated equilibrium potentials. Overpotentials would arise. As discussed by Macdonald and Owen, in the presence of overpotentials, the potential arrests would tend to be more cathodic for a cathodic scan and more anodic for an anodic scan relative to the calculated equilibrium potential which neglects overpotentials.

These studies at high pH indicate that a detectable phase of $\text{Fe}(\text{OH})_2$ can be formed at potentials and pH consistent with those shown in Figures 2 and 3. Such results suggest that $\text{Fe}(\text{OH})_2$ may be formed at lower pH values. The predicted existence of dissolved $\text{Fe}(\text{OH})_2$ suggests that solid $\text{Fe}(\text{OH})_2$ can dissolve (corrode) slowly. The diagram for iron revised to show solid and dissolved $\text{Fe}(\text{OH})_2$ by using the newer thermodynamic data is consistent with experimental observations.

References

1. M. Pourbaix, Atlas of Electrochemical Equilibria in Aqueous Solutions, p. 307, Cebelcor, NACE, Houston (1974).
2. M. Cohen. Dissolution of Iron, in Corrosion Chemistry, R. F. Gould, ed., ACS Symposium Series 89, American Chemical Society, Washington, D. C. (1979).
3. C. F. Baes and R. E. Mesmer. The Hydrolysis of Cations, 3rd, John Wiley and Sons, New York (1976).
4. G. B. Naumov, B. N. Ryzhenko, and I. L. Khodavsky. Handbook of Thermodynamic Data, USGS-WRD-74-001 Eng. Trans (1974).
5. M. H. Fronig, M. E. Shanley, and E. D. Verink, Corros. Sci., Vol. 16, p. 371 (1976).
6. F. A. Cotton and G. Wilkinson, Advanced Inorganic Chemistry, John Wiley and Sons, New York, 1980.
7. F. H. Sweeton and C. F. Baes. J. Chem. Thermodynamics, Vol. 2, p. 459 (1970).
8. P. R. Tremaine and J. C. LeBlanc. J. Solution Chem., Vol. 9, No. 6, p. 415 (1980).
9. Y. Geronov, T. Tomov, and S. Georgiov. J. Appl. Electrochem., Vol. 5, p. 351 (1975).
10. D. D. Macdonald and D. Owen. J. Electrochem. Soc., Vol. 120, No. 3, p. 317 (1973).
11. D. Geana, A. A. El Miligy, and W. J. Lorenz. J. Appl. Electrochem., Vol. 4, p. 337 (1974).
12. R. D. Armstrong and I. Baurhoo. J. Electrochem. Soc., Vol. 34, p. 41 (1972).
13. A. M. Coutre and K. J. Laidler. Canadian J. Chem., Vol. 35, p. 202 (1957).